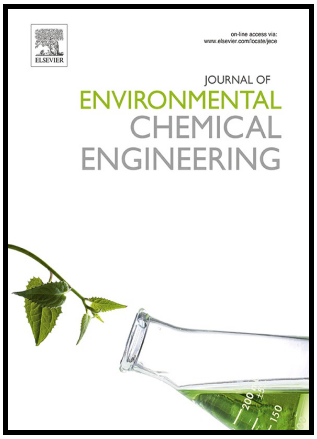

Downflow Bubble Column Electrochemical Reactor (DBCER): *In-situ* production of H_2O_2 and O_3 to conduct Electroperoxone Process

Germán Santana-Martínez, Gabriela Roa-Morales, Leobardo Gómez-Olivan, Ever Peralta-Reyes, Rubí Romero, Reyna Natividad

PII: S2213-3437(21)00125-1

DOI: https://doi.org/10.1016/j.jece.2021.105148

Reference: JECE105148

To appear in: *Journal of Environmental Chemical Engineering*

Received date: 26 November 2020
Revised date: 13 January 2021
Accepted date: 29 January 2021

Please cite this article as: Germán Santana-Martínez, Gabriela Roa-Morales, Leobardo Gómez-Olivan, Ever Peralta-Reyes, Rubí Romero and Reyna Natividad, Downflow Bubble Column Electrochemical Reactor (DBCER): *In-situ* production of H_2O_2 and O_3 to conduct Electroperoxone Process, *Journal of Environmental Chemical Engineering,* (2020) doi:https://doi.org/10.1016/j.jece.2021.105148

Downflow Bubble Column Electrochemical Reactor (DBCER): *In-situ* production of H_2O_2 and O_3 to conduct Electroperoxone Process

Germán Santana-Martínez[a], Gabriela Roa-Morales[a,*], Leobardo Gómez-Olivan[b], Ever Peralta-Reyes [c], Rubí Romero, Reyna Natividad[a,*]

[a]Centro Conjunto de Investigación en Química Sustentable UAEM-UNAM, Universidad Autónoma del Estado de México, Km. 14.5 carretera Toluca-Atlacomulco, Toluca, Estado de México, Mexico.

[b]Facultad de Química, UAEM, Paseo Tollocan esq Paseo Colon C.P 50120, Toluca, Estado de México, Mexico.

[c]Universidad del Mar, Campus Puerto Ángel, Ciudad Universitaria S/N, C. P.70902, Puerto Ángel, Oaxaca, Mexico.

*Corresponding authors: rnatividadr@uaemex.mx (R. Natividad), groam@uaemex.mx (G. Roa)

Highlights

- DBCER allows to conduct E-peroxone with *in situ* reagents production.
- O_3 and H_2O_2 are produced *in situ* with BDD and used to mineralize phenol.
- DBCER reduces reagents consumption and eliminates gas waste.
- Electro-peroxone of phenol at pH 7 eliminates toxicity on *Cyprinus carpio*.

Keywords

- Advanced Oxidation Processes
- Electro-peroxone.
- BDD anode/cathode.
- Mineralization
- Phenol Toxicity

Abstract

In the context of water remediation, advanced oxidation processes have been proven to be an effective solution. In most of the cases, however, the reaction systems are usually highly expensive, because of the addition of chemical substances or energy consumption. This usually constrains their application at an industrial scale. This has motivated several researchers to develop technologies able not only to intensify the processes but able also to increase the sustainability of the whole process. In this context, this work aimed to assess a relatively novel technology, a Downflow Bubble Column Electrochemical Reactor (DBCER), in the mineralization of a rather typical organic pollutant, phenol.

The studied variables were: current density (20-60 mA/cm^2), electrolyte concentration (0.025-0.1 M), liquid recirculation rate (4.7 and 6 L/min) and pH (3 and 7). The response variables were total organic carbon (TOC), phenol and by-products concentration, oxidant species concentration (O_2, H_2O_2 and O_3).

It was demonstrated that the DBCER with BDD electrodes allows not only the production of $^{\bullet}OH$, but also the *in situ* production of O_2, H_2O_2 and O_3 (without the addition of any gas) and more importantly their utilization to conduct an electro-peroxone process.

The highest mineralization degree was around 75 % under pH 3, 60 mA/cm^2, 4.7 L/min and an electrolyte concentration of 0.05 M. Under these conditions, it was figured out that the phenol oxidation occurs mainly by ozone attack and the main remaining compound was oxalic acid. Although at pH 7 the mineralization degree was lower than at pH 3, it was demonstrated by a biotoxicity study on *Cyprinus carpio* that the original toxicity was significantly decreased.

1. Introduction

Electrochemical Advanced Oxidation Processes (EAOP) have become of paramount importance in the context of water remediation [1]. Despite their proven efficiency, and in the context of sustainability, research on this topic is still needed since there remain challenges to be addressed like energy consumption, scaling-up, process intensification to reduce the treatment time and minimization of operating costs, mainly. An important strategy is the improvement of existing processes by minimizing the addition of chemical reagents and the discharge of waste to the environment. In this sense, since some years ago, several researchers have focused on the improvement of the peroxone process [2] that mainly consists on the generation of strongly oxidant species by the reaction of hydrogen peroxide with ozone,

$$2H_2O_2 + 2O_3 \rightarrow H_2O + 3O_2 + HO_2^{\bullet} + OH^{\bullet} \quad (1)$$

Conventionally, the two reagents are added to the reaction system, the first with commercial H_2O_2 and the second one supplying oxygen to an ozone generator to produce it. Lately, however, H_2O_2 *in-situ* electrochemical production has been widely reported by using carbonaceous materials as electrodes [3,4]. This has been mainly applied to carry out electro-fenton and electro-peroxone processes that consist on conducting reaction 1 but with electrogenerated hydrogen peroxide by reduction of oxygen at the cathode,

$$O_{2(g)} + 2H^+ + 2e^- \rightarrow H_2O_2 \quad (2)$$

This reaction has also been reported to occur with boron doped diamond electrodes (BDD) [5,3].

The increase in the use of the electro-peroxone process has been motivated by the following advantages in the mineralization of pollutants [6–9]:

- Accelerates the transformation of O_3 to $^{\bullet}OH$ [10].
- The addition of H_2O_2 and O_3 does not generate polluting by-products, only H_2O and O_2 [11,12].
- Reduced formation of bromates and bromide (compounds potentially carcinogenic) in effluents[13,14].
- The process efficiency is increased, and the energy demand is decreased, this is because the treatment time is shorter with respect to the separate processes. Also, it is a safer option with lower costs [9].
- Enhances the abatement kinetics of ozone resistant pollutants [15] .

Nevertheless, in a typical electro-peroxone process the external production and addition of O_3 still is a common practice and represents an opportunity of improvement not only from the chemical point of view but also from an economical angle. In this sense, recently, the simultaneous generation of ozone and peroxide at neutral pH has been reported and this eliminates the implementation of an ozone generator, which saves the costs of the process. This reaction system was implemented using a carbon PTFE cathode and as anode a membrane electrode assembly (MEA) [16] and the following reactions were reported to be the via of reagents production,

$$Cathode\ 1.5O_2 + 6H^+ + 6e^- \rightarrow 3H_2O \quad (3)$$

$$Anode\ 3H_2O \rightarrow 6H^+ + 6e^- + O_3 \quad (4)$$

In the context of BDD electrodes application, however, since more than a decade ago is known that ozone is produced in the electro-oxidation process, in similar way to the abovementioned system [17]. The typical cells to achieve so, however, are not able to retain

the produced gas within the system and therefore the generated O_3 is underutilized since it is only given a rather limited contact time with the reacting solution. In this sense, it is desirable to have a reactor that allows to overcome such a drawback.

Because all the aforementioned, it was the main objective of this work to assess the performance of a Downflow Bubble Column Electrochemical Reactor (DBCER) equipped with BDD electrodes in the *in-situ* and simultaneous production of H_2O_2 and O_3 to conduct an oxidation process. This type of bubble column, albeit without electrodes, has been successfully applied to conduct gas absorption, photo-catalyzed processes and hydrogenation reactions [18–20]. Among its main documented advantages are the high gas-liquid volumetric mass transfer coefficients and a 100% gas utilization by maintaining the bubble dispersion within the reaction zone.

A conventional operation of this bubble column implies the simultaneous injection on the top of the reactor of the two-phase, gas and liquid. In this proposal, however, no gas is fed into the reactor, but oxygen and ozone are electro-generated *in situ* as well as hydrogen peroxide. To test the efficiency of this electrochemical reactor, phenol was used as a model molecule, which is a highly persistent pollutant and is found as a raw material or typical by-product of degradation in the chemical industry. A biotoxicity assay of the treated effluent is also presented.

2. Materials and methods

2.1 Chemicals

A phenol standard (99.5% purity) purchased from Merck was used to prepare the solutions for experimentation and for HPLC analysis. Sodium sulfate (Na_2SO_4) provided by Reasol was used for the preparation of the electrolyte solution. In some cases, the solutions were adjusted to a specific pH, employing solutions of NaOH or H_2SO_4 [1M], both reagents were supplied by Fermont. With respect to chromatographic analysis, the mobile phases were prepared with methanol HPLC grade, purchased from Fermont. Potassium phosphate monobasic (K_2HPO_4) and ortho-phosphoric acid (H_3PO_4 85%) purchased from J.T Baker and Merck, respectively, were used to prepare the buffer solution. To quantify the hydrogen peroxide concentration evolution with time, a titanium sulfate solution was prepared by the reaction between TiO_2 (Degussa) and H_2SO_4 [21]. To determine the ozone concentration, a solution with phosphate monobasic, ortho-phosphoric acid and potassium indigotrisulfonate supplied by Sigma Aldrich, was prepared [22]. All solutions for calibration were prepared with deionized water.

2.2 Downflow Bubble Column Electrochemical Reactor (DBCER)

This reaction system is shown in Figure 1. The DBCER is a cylindrical undivided cell made of borosilicate, the volume is 2.0 L with an internal diameter of 5 cm and 100 cm of length, and a couple of electrodes of Boron Doped Diamond (BDD manufactured by CONDIAS) with 50 cm^2 of active area. The dimensions of each electrode were 20 cm x 2.5

cm. At the top flange there is a small orifice (4 mm) that exerts a Venturi effect on the entering phases (electrolyte solution that is being recirculated). Because of the high energy at which the liquid enters the reactor, the generated gas at the electrodes is broken down and a matrix of small bubbles is generated thus increasing turbulence, contact area and mass transfer between gas-liquid-solid (electrodes). In addition, and unlike up-flow bubble columns, the arrangement proposed here offers the advantage of keeping the gas phase in contact with the liquid phase at all times. Also, because the cell is fully flooded with liquid, the length of electrodes is a plausible variable to be studied as well as the surrounding hydrodynamics (one or two-phase). This implies a near to 100% utilization of the either input or generated gas. In this reactor, the bubble matrix height depends on the inlet liquid velocity (at the inlet orifice), the coalescing characteristics of the system, gas production and consumption rate, pressure and temperature. In order to initiate and maintain the dispersion of the gas into the liquid and produce a stable bubble matrix, a minimum inlet velocity must be established. In this work, it was experimentally determined to be 6.23 m/s (given by the 4.7 L/min liquid flowrate). This inlet velocity ensures the gas will not accumulate on top of the column in the range of studied variables for this system.

It is observed in this type of reactors, that the gas bubble size increases along the axial direction due to coalescence. At the maximum bubble dispersion height (~ 0.3 m) the Sauter mean diameter of the bubbles was found to be 0.8×10^{-3} m. To establish this value, a millimetric scale was sticked to the column and images were taken with a Camera Fuji 300. The size of 30 bubbles per image was then obtained and the mean Sauter diameter was calculated. This diameter was not found to significantly vary within the range of the studied variables. This is an important value in order to calculate the bubble rise velocity which dictates the maximum liquid velocity in order to maintain the bubble dispersion within the reactor. If the liquid velocity in the reactor is higher than the bubble rise velocity, then the bubbles are carrying away from the reactor and the gas in underutilized. Thus, this is not a recommended operating mode. In our case, the maximum liquid flowrate (6 L/min) provided by the pump allowed the coalesced bubbles to rise up to the top where they were breaking down again into small bubbles by the hydrodynamic effect of the high inlet velocity, thus allowing to maintain the bubble dispersion.

The gap between electrodes used in this study was 8×10^{-3} m at all experiments. Current density was controlled by a power supply EXTECH 1683. The oxygen generated *in situ* by BDD electrolysis was on-line monitored by an oxygen analyzer HACH 400. At the same time, ozone was *in situ* generated with the oxygen produced by electrolysis. At the end of the process, the unconsumed ozone was sent to a device called ozone destroyer (manufactured by Pacific Ozone Technology). The gas purge line was placed on top of the column (see figure 1), thus, the valve right below the Ozone destroyer was opened in order to purge any remained gas.

The pipelining, valves, tank and cooler were fabricated of stainless steel. To recirculate the solution in the system a WEG centrifugal pump of 1 HP was employed. The pump used to recirculate the solution, transfers heat to the solution and this is an advantage if temperature

was a variable to be assessed. Nevertheless, a cooling system was necessary to conduct experiments at constant temperature. For this purpose, a Rotoplas^{RM} centrifugal pump of 0.5 HP, was coupled to a cooling tank to control temperature.

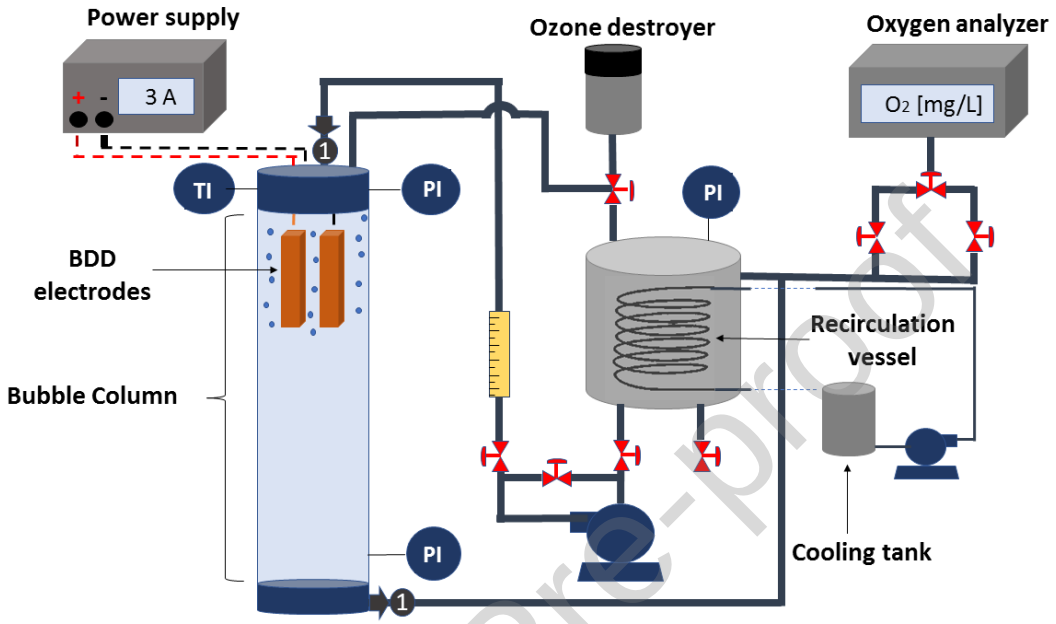

Figure 1. **Downflow Bubble Column Electrochemical Reactor (DBCER)**

2.3 Phenol Oxidation

In order to establish the feasibility of conducting oxidation processes in the DBCER, phenol removal was studied.

First of all, the conductive-diamond electro-generation of O_2, H_2O_2 and O_3 was studied without the addition of phenol. For this purpose, only water (from the mains) was employed. This water had an initial TOC of 35 mg/L, initial O_2 concentration of 5.9-6.5 mg/L, pH_0 (7.4-8.1) and conductivity (950-983 µS). This study was conducted under a liquid recirculation rate of 4.7 L/min and the effect of current density (20, 40 and 60 mA/cm^2) and pH (3, 7 and without control) was established.

For the study of phenol removal, 100 mg/L phenol solutions were prepared and for that purpose mains water was used at all times. The studied variables were liquid recirculation flowrate (Q_L), electrolyte concentration and pH. Current density was kept constant at all times at 60 mA/cm^2. The effect of Q_L was investigated at two levels, 4.7 and 6 L/min. At these liquid flowrates, the liquid velocity was enough to maintain a bubble dispersion without gas accumulation on the top of the column and without bubbles being carried away from the reactor. The study of the effect of liquid flowrate was carried out only at acidic conditions (pH=3) and with an electrolyte concentration of 0.05 M. When studying the

effect of electrolyte concentration, the acidic conditions were maintained and the lowest flowrate was employed. Finally, the effect of pH (3 and 7) was studied and for this purpose the other reaction conditions were elected according to the highest attained TOC removal, i.e. Q_L=4.7 L/min, [electrolyte]=0.05 M and J=60 mA/cm^2. At all cases the response variables were total organic carbon (TOC) removal and phenol concentration (when added). Phenol oxidation by-products concentration and conductive-diamond electrogenerated species concentration (O_2, H_2O_2 and O_3) were also established when studying the effect of pH. Temperature was 23°C ± 2 at all experiments. Although the reactor design allows to conduct the experiment at pressures in the range of 0 – 4 bar, all experiments were conducted at an absolute pressure of 0.74 bar.

2.4 Analytical procedures

The mineralization degree was established by the quantification of Total Organic Carbon (TOC) with a Shimadzu TOC-L analyzer by injecting aliquots of 50 µL per sample. Regarding pH, this variable was monitored by a Fischer Scientific TB-150 pH-meter.

An UHPLC Vanquish diode array detector (Thermo Scientific) was used to quantify the phenol and its oxidation by-products (Aromatic compounds and carboxylic acids). The used software was Chromeleon 7.2. In this analytical procedure, the injection volume was 5 µL and temperature was controlled at 25°C to conduct the chromatography in isocratic mode. For the analysis of aromatic compounds, a column Ascentis Express C-18 (Supelco), 3.0 cm in length and 4.6 mm in diameter, was used. The mobile phase was Methanol/H_2O_2 (20:80 v/v and 5mM H_2SO_4) at 1.0 mL/min. Regarding wavelength, this was set at 246, 270 and 280 nm. The rest of by-products were separated by a ZORBAX Eclipse XDB C-18 (Agilent) column, 15.0 cm in length and 4.6 mm in diameter, employing a buffer solution as a mobile phase of Methanol/H_2O_2 (10:90 v/v) and 30 mM K_2HPO_4 adjusted at pH 2.5 with H_3PO_4. This solution was pumped at 0.5 mL/min and the wavelength was s et at 210 nm.

To quantify the amount of hydrogen peroxide, an aliquot from reaction solution was treated with titanium sulfate and then analyzed at λ: 408nm [21]. At the same time, other sample was taken to determine ozone concentration employing Potassium indigotrisulfonate at λ: 600 nm [22]. Both spectroscopic determinations were conducted with a PerkinElmer Model Lambda 25 UV/Vis spectrophotometer using a quartz cell with 1 cm of optical path.

The percentage of mineralization efficiency (MCE%) was estimated for each studied variable with the following equation,

$$MCE(\%) = \frac{nFV_s\Delta(TOC_i - TOC_f)}{4.23x10^7\ m\ I\ t} * 100 \quad (5)$$

where n is the number of consumed electrons, considering that phenol is mineralized as follows,

$$C_6H_6O + 11H_2O \rightleftharpoons 6CO_2 + 28\,H^+ + 28\,e^- \quad (6)$$

F is the Faraday constant (96487 C•mol^{-1}), V_S is the treated solution volume in liters (L),

$\Delta(\mathrm{TOC_i} - \mathrm{TOC_f})$ is the experimental TOC change in the treatment time t (h), TOC_i= initial TOC, TOC_f= final TOC, 4.32 x10^7 is a conversion factor to homogenize units (=3600s•h^{-1}, 12,000 mg carbon•mol^{-1}), m, is the number of carbon atoms in the molecule (6 atoms),

I, is the applied current (Amperes).

The energy consumption per unit of removed TOC was calculated also for each studied variable with the following equation,

$$EC(kWh(gTOC)^{-1}) = \frac{E_{cell}\ \mathrm{It}}{V_s\ \Delta(TOC_i - TOC_f)} * 100 \quad (7)$$

where E_{cell} is the applied voltage.

2.5 Biotoxicity study

In order to establish the biological efficiency of the treatment conducted at pH 7 in the DBCER, sub-lethal toxicity tests on fish were conducted. For this purpose, two biomarkers were employed, i.e. 1) single-cell gel electrophoresis (comet assay) and 2) Micronuclei assay. Both tests were conducted on erythrocytes of the test specimens.

The acquisition and adaptation of test organisms, sub-lethal toxicity assays, the comet and the micronuclei assays are described in detail in the Supplementary Material 1 (S1).

3. Results and discussion

3.1 Conductive-diamond electro-generated O_2, H_2O_2 and O_3

As starting point, the concentration of *in situ* electro-generated oxidant species in a blank solution (without adding phenol) was established. Such species were hydrogen peroxide, oxygen and ozone at different reaction conditions. Figure 2 depicts the concentration profiles of each oxidant in the current density range of 20 – 60 mA/cm^2, recirculation flowrate of 4.7 L/min, electrolyte concentration of 0.05 M Na_2SO_4 and pH=3. In order to study the distribution of oxidant species, phenol was not added. The results of similar experiments, at pH=7 and without pH control though, are presented in the supplementary material S2.

In all cases, the water used in these tests has an associated initial oxygen concentration (5.9-6.5 mg/L). Nevertheless, when a current density is applied, oxygen concentration tends

to increase (see figure 2 and S2.1 and S.2.2) and this can be ascribed to the side reaction of oxygen evolution that can be represented as follows [23],

$$2H_2O \rightarrow O_2 + 4H^+ + 4e^- \quad (8)$$

In conventional electrochemical cells, the oxygen generated from reaction (8) is typically released to atmosphere. Advantageously enough, the DBCER not only allows to keep this gas inside the reactor but also to efficiently disperse it into the electrolyte to maximize its use and consumption. As can be seen from Figure 2, oxygen concentration increases with respect to the initial value up to 9 mg/L. Although oxygen evolution does not favor the formation of hydroxyl radicals, this gas can be transformed to ozone and hydrogen peroxide. The latter is expected to be produced at the cathode by oxygen reduction according to reaction (2) and it is also formed by the addition of two hydroxyl radicals, as observed in reaction (9) [4],

$$OH^\bullet + OH^\bullet \rightarrow H_2O_2 \quad (9)$$

On the other hand, ozone can be produced by water electrolysis according to the following reaction [24],

$$3H_2O \rightarrow O_3 + 6H^+ + 6e^- \quad (10)$$

To obtain this reaction (10), specifically with BDD electrodes, several authors have documented and proposed a mechanism based on the following reactions [24],

$$H_2O \rightarrow OH^\bullet + H^+ + e^- \quad (11)$$

$$OH^\bullet \rightarrow O^\bullet + H^+ + e^- \quad (12)$$

$$2O^\bullet \rightarrow O_2 \quad (13)$$

$$2\mathrm{OH}^{\bullet} \rightarrow H_2O_2 \quad (14)$$

$$H_2O_2 \rightarrow O_2 + 2H^+ + 2e^- \quad (15)$$

$$O_2 + O^{\bullet} \rightarrow O_3 \quad (16)$$

As can be observed in reaction 15, the hydrogen peroxide is decomposed to oxygen and protons. This may explain why oxygen concentration increases even when ozone is being produced and also why hydrogen peroxide is not appreciable. It is also plausible that the hydrogen peroxide could be reacting with the produced ozone as follows [11],

$$H_2O_2 + O_3 \rightarrow {}^{\bullet}OH + {}^{\bullet}O_2^- + O_2 \quad (17)$$

This reaction not only would explain the increase in oxygen concentration but also explains the minimum quantified amount of H_2O_2 when phenol is not added. This phenomenon has also been previously reported [11] .

Despite the O_3 consumption by reaction 17, it is worth noticing that ozone concentration was practically constant (5 ± 0.5 mg/L) during the whole experiment, excepting at pH 3 and 60 mA/cm^2, where ozone concentration decays down to 2.9 mg/L.

It is worth clarifying that even when phenol was not added, the initial TOC of the electrolyte solution for this study was 35 mg/L. This is due to the electrolyte solution being prepared with mains water. Thus, TOC analyses were also conducted in this blank experiment at the beginning and after 6 h of electrolysis. The results show a reduction of 40% and 55% when current densities of 20 mA/cm^2 and 40 mA/cm^2 were applied, respectively. However, the highest removal value (98%) was obtained with a current density of 60 mA/cm^2. This can be associated with the increase of hydroxyl radicals production and the presence of protons which facilitates to maintain the acidic media via the following reaction [25],

$$\mathrm{BDD} + H_2O \rightarrow BDD(\mathrm{OH}^{\bullet}) + H^+ + e^- \quad (18)$$

Furthermore, only under these experimental conditions, pH=3 and 60 mA/cm^2, the ozone concentration decays from 5 ± 0.5 mg/L to 2.9 mg/L (see figure 2). This behavior and the high TOC removal achieved under these conditions, suggest that the ozone participation in

the mineralization of the solution increases in this might be due to oxidation route 1 (see figure 9).

The obtained results regarding TOC removal in the blank solution, are a clear indicative that in acidic media and with high current densities, the concentration of the *in-situ* produced oxidants is enough to eliminate the organic matter from water. It should also be kept in mind that at high current densities, the amount of hydroxyl radicals is also expected to increase by reaction (18) and thus the direct oxidation over the electrodes surface by means of reaction 19,

$$BDD(OH^{\bullet}) + R \rightarrow BDD + CO_2 + H_2O + H^+ + e^- \qquad (19)$$

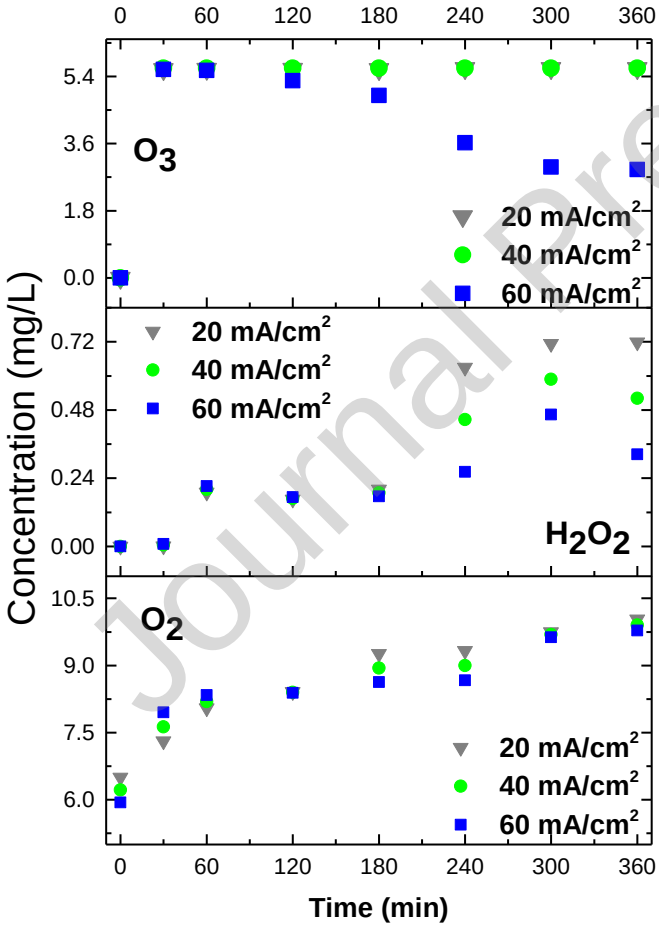

Figure 2. Effect of current density on conductive-diamond electro-generation of O_2, O_3, H_2O_2. Operating conditions: pH=3, 0.05 M [Na_2SO_4], T: 23°C ±2, $[Ph]_o$=0 mg/L, Q_L= 4.7 L/min.

3.2 Phenol oxidation: Effect of Recirculation flow-rate and electrolyte concentration

In the previous section, the quantification of oxygen, hydrogen peroxide and ozone demonstrated that is possible to generate them simultaneously *in-situ* and to keep them inside the electrochemical reactor and use them to mineralize organic matter, thus showing the feasibility of conducting an electro-peroxone treatment without the external addition of ozone or hydrogen peroxide but generating them *in situ*. Nevertheless, it was decided to add phenol in order to fully demonstrate the capabilities of the assessed technology.

The effect of recirculation flowrate (Q_L) on normalized TOC is shown in Figure 3. These results show a significant lower TOC removal rate when maximum recirculation flowrate is applied. Reynolds number (Re) and residence time (τ) were calculated for every liquid flowrate within the column reactor. At 4.7 L/min, Re was 2131 and τ was 25 s. These parameters were 2721 and 19.6 s for 6 L/min. These Re numbers were calculated with the liquid velocity in the electrodes area and the residence time refers to the time that the liquid spends in the column per pass (keep in mind that the liquid is under constant recirculation). Thus, in terms of TOC removal, it can be concluded that is more beneficial to increase residence time rather than turbulence, i.e. Re number.

The effect of electrodes location (top and bottom) within the DBCER was also studied. The results are shown in figure S2.3. It can be observed that locating the electrodes at the top of the column provides better results in terms of TOC removal rate and this was the reason to carry out all the experiments with the electrodes placed at the top. Placing the electrodes at the bottom of the column does not eliminate the presence of the gas phase because this is where it is being produced. It was observed, however, that at this location, only the rise of the bubbles occurs without the intense mixing that it is observed when the electrodes are placed at the top. This might be the reason for the lower performance observed when the electrodes are placed at the lowest part of the DBCER.

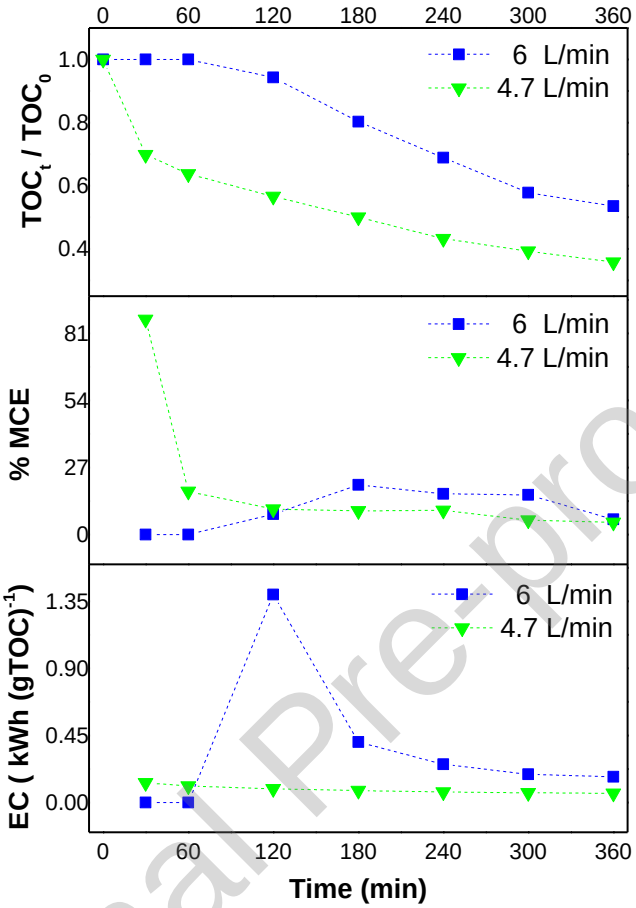

Figure 3. Effect of recirculation liquid flow-rate on normalized TOC, mineralization efficiency percentage (%MCE) and energy consumption (EC). Reaction conditions: $[Phenol]_0$= 100mg/L, $[TOC]_0$= 118 mg/L, pH=3, j=60 mA/cm^2, 0.05 M [Na_2SO_4], V= 3.5 L and T= 23°C ±2.

Another important aspect of the process is the electrolyte concentration, since it is directly related to the solution conductivity and the generation of oxidant species. Regarding this variable, the preferable value in Electro-Fenton and Electro-Oxidation is 0.05 M of sodium sulfate [25,27–29], only in few investigations this value has been increased to 0.1 M [30]. In this work, the effect of this variable on normalized TOC was assessed in the range of 0.025-0.1 M and the results are shown in Figure 4. It is well known that the solution conductivity is directly related to the concentration of supporting electrolyte, in this case with the value of 0.025 M, less TOC was removed (20% less) than when a 0.05 M sodium sulfate electrolyte solution was used. However, when this value is duplicated, *i.e.* when a 0.1M sodium sulfate electrolyte solution was used, the TOC removal decreases 3%. This indicates that a high sodium sulphate concentration does not aid mineralization, despite of the already reported disinfecting effect of sulphates [23]. The addition of sulphuric acid to

keep pH=3, promotes the generation of sulphate radicals and peroxodisulphate by the following reactions [23],

$$SO_4^{-2} + OH \rightarrow SO_4^{-} + OH^{-} \quad (20)$$

$$2HSO_4^{-} + OH \rightarrow S_2O_8^{2-} + 2H_2O \quad (21)$$

These species are reactive oxygen species (ROS), albeit their standard potential is lower than O_3, H_2O_2 and $OH^{\bullet}$. Therefore, the excess of sulphate ions inhibits the action of OH radical by reacting like scavengers of other mediators [23]. Considering this, it is very important to establish an ideal concentration of supporting electrolyte to generate high amounts of ROS with high standard potential and minimize reagent consumption. In this case, it can be observed that the best concentration of electrolyte in terms of TOC removal rate is 0.05M. Therefore, this concentration was used for the remained experiments and is in concordance with previous investigations.

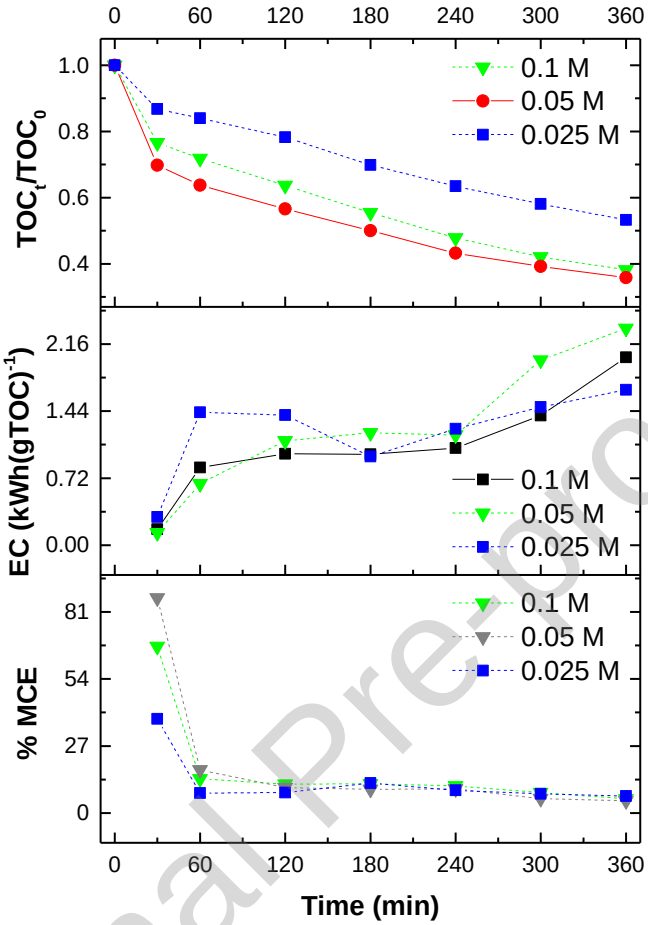

Figure 4. Effect of electrolyte concentration [Na_2SO_4] on normalized TOC, mineralization efficiency percentage (%MCE) and energy consumption (EC). Reaction conditions: $[Phenol]_0$:100mg/L, pH=3, *j*=60 mA/cm^2, Q_L: 4.7 L/min, $[TOC]_0$: 118 mg/L, V: 3.5L and T: 23°C ±2.

Figures 3 and 4 also show the effect of liquid flowrate and electrolyte concentration on the percentage of mineralization efficiency and energy consumption. Regarding the former, the results confirm that the best conditions to conduct the phenol mineralization are Q_L= 4.7 L/min, [Na_2SO_4]=0.05 M. Under these conditions, the usage of the consumed current is 85% at a treament time of 30 minutes and this can be mainly attributed to the produced oxidant species. After this time, the mineralization efficiency significantly decreases and this might be due to the increased concentration of the oxidation by-products. This will be discussed in more detail in section 3.3.

In terms on energy consumption (EC), it can be observed in figure 3, that the EC is lower at the lowest liquid flowrate. This was expected because of the higher mineralization observed

at 4.7 L/min. In figure 4, it is observed that there is not an apreciable effect of electrolyte concentration in the range of 0.05 M and 0.1 M on EC in the first 240 minutes.

3.3 Phenol oxidation: effect of pH

Figure 5 shows the effect of pH on normalized TOC. It can be observed that after 6 hours of treatment the maximum attained TOC removal was 75% at pH=3 and 65% at pH =7. None of these values are at stationary state though, meaning that the longer the treatment the higher the attained TOC removal. It can be observed in figure 5 that, as expected, these profiles depend on both, pH and time. At acidic conditions, two main stages are distinguished. The first one lasts for about 30 minutes and only in this time about 35% of the total TOC content is removed. In the following 5.5 h of treatment, however, TOC removal dramatically slows down and only a further 40% is removed. In order to explain this phenomenon, the phenol and oxidation by-products concentration profiles with time were obtained and these are shown in figures 6 and 7a. It can be observed in figure 6, that in the first 30 minutes, 25% of phenol was removed. During this time, however, the only appreciable by-product is maleic acid at pH=3 (see figure 7 a). A longer treatment time under acidic conditions leads to obtain aromatic compounds (catechol, hydroquinone, benzoquinone) and acids (maleic, malonic, fumaric and oxalic). It can also be observed in figure 7a, that all by-products but oxalic acid are further degraded at some point of the treatment. Thus, it can be concluded that the first stage observed in the TOC removal profile at pH=3 (figure 5) is due to the phenol degradation following the sequence maleic acid (by cleavage of the aromatic ring by an electrophilic attack of molecular ozone), fumaric and malonic acids and then their oxidation towards CO_2 and water. In this sense, it has been reported [31] that double-bond acids readily react with ozone via Criege's mechanism. It is worth noticing that hydrogen peroxide has been reported [32] as one of the products when the aromatic ring is destroyed to produce maleic fumaric acids by molecular ozone attack. The electrophilic attack of ozone to the phenol molecule has also been reported [31,32] to lead to hydroxylation products, i.e. catechol and hydroquinone, which are further oxidized towards benzoquinone, oxalic acid and CO_2 and water. It can also be observed in Figure 7a that oxalic acid accumulates, and, unlike the aromatics, it is not further oxidized. This is something expected in an ozonation treatment since the nucleophilic reaction of ozone with a carboxyl group is rather slow [31]. Thus, it can be concluded that the slowing down of the TOC removal profile (after 30 min) can be ascribed to the prevalence of direct oxidation by molecular ozone and the appearance of hydroxylation products and compounds with carboxyl groups. This does not rule out the oxidation by hydroxyl radicals and the other oxidant species though. Therefore, the oxidation products at pH=3 shown in figure 7a, are the result of all the produced oxidant species. The TOC removal percentage (35%) after 30 minutes of treatment (see figure 5) is evidence of this.

According to figure 5, phenol is also mineralized at pH 7 albeit with a rather different behavior than at pH 3. Unlike at pH 3, in this case the TOC profile exhibits three rate stages, the first one lasts for 60 minutes and no mineralization at all is observed ($-r_{TOC}=0$).

The second stage lasts for further 180 minutes and its removal rate is rather similar to the second stage of TOC profile at pH=3. A third stage, with a clear higher removal rate, is observed after 240 minutes. All this and the products distribution (figure 7b) suggest a different oxidation mechanism prevailing at pH=7.

With the results shown in figure 6, the kinetic parameters for phenol oxidation were estimated. At both pH, 3 and 7, the reaction was pseudo-first order and the specific rate constants are of the same order of magnitude ($k = 0.0187\ min^{-1}$ at pH=3 and $k= 0.0119\ min^{-1}$at pH=7). This result was unexpected since pH has been reported (although not in an electrochemical process) to positively affect phenol removal not only because of ozone decomposition but because of phenol dissociation leading to the appearance of phenolates [31]. In this case, despite the similarity in specific rate constants, the products distribution at pH 7 (figure 7 b) show that the main accumulated compounds are hydroxylation products that build up during the first 60 minutes. Phenol oxidation then might be occurring by oxidant radicals attack rather than by molecular ozone. Also, it should be kept in mind that in this system O_3 is not being fed at anytime but *in situ* produced. This fact along with the contact time, might be limiting the oxidants species concentration, mainly the hydroxyl radicals concentration, which seems to be increasing with time and this is suggested, once again by the products distribution, since after 120 and 180 minutes, the hydroxylation products, i.e. hydroquinone, catechol and benzoquinone, readily decay. This decay is related to the presence of more hydroxyl radicals evidenced by a decrease in H_2O_2 concentration (figure 8) and thus suggesting the prevailing phenol and by-products oxidation mechanism at pH=7 is via an electro-peroxone process (reaction 1). Thus, at this pH, O_3 is mainly being used to react with H_2O_2 and to produce hydroxyl radicals that are able to oxidize carboxylic compounds, and this explains the less extent of accumulation of oxalic acid compared to pH=3 (see figure 7). In neutral media, carboxylic acids remain in deprotonated form and with this condition is easier to destroy this kind of molecules [11], this is not applied to all cases and also has been reported that some molecules are easier to be removed in acidic rather than in neutral media [33].

Regarding energy consumption, this is lower at pH 3 than at pH 7 (see figure 5) until 240 minutes. After this time the EC at pH=7 becomes lower than at pH=3. This can be ascribed to the prevailing mechanism and the oxidation by-products. As aforementioned, the products distribution and the identified oxidant species at pH=3, suggest that not only the hydroxyl radicals are responsible for the oxidation but mainly the electrochemically produced ozone. After 240 minutes, it is observed in figure 5 that the remaining oxidation by-products are mainly carboxylic acids, which are rather reluctant to the attack of molecular ozone and therefore the mineralization is diminished. This implies an increase on EC. It is very likely, however, that at a longer treatment time, such carboxylic acids eventually will be degraded by the hydroxyl radicals at the BDD surface and in the liquid bulk, as observed at pH=7. The above explained also impacts the percentage of mineralization efficiency plotted in figure 5. This parameter finds its maximum (85%) at pH=3 after 30 minutes of treatment and is 28% at pH=7 after 360 minutes of treatment.

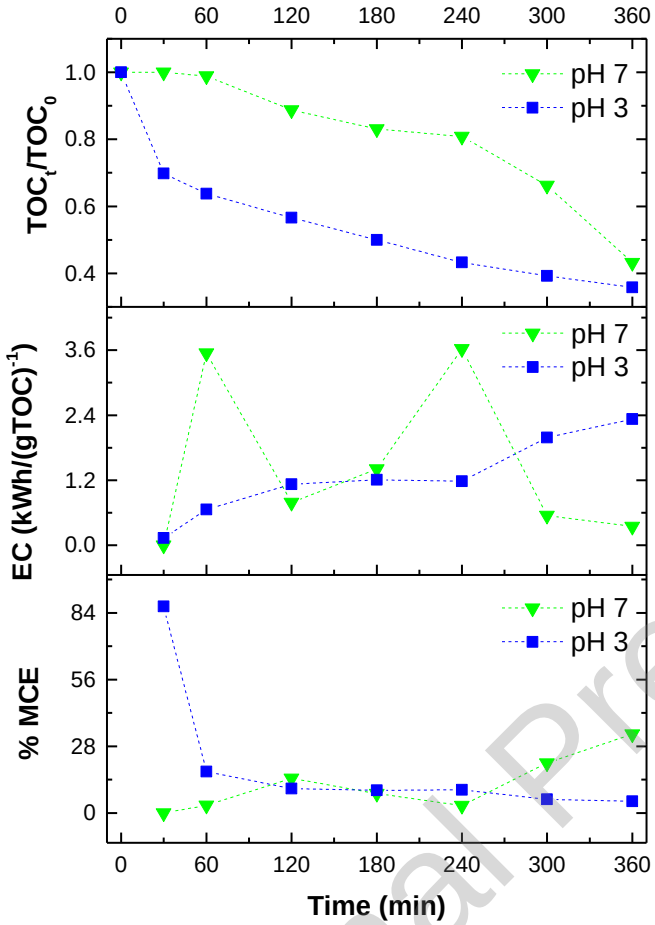

Figure 5. Effect of pH on normalized TOC, mineralization efficiency percentage (%MCE) and energy consumption (EC). Reaction conditions: $[Phenol]_0$:100 mg/L, 0.05 M $[Na_2SO_4]$, j=60 mA/cm^2, Q_L= 4.7 L/min, $[TOC]_0$: 118 mg/L, V=3.5L and T= 23°C ±2.

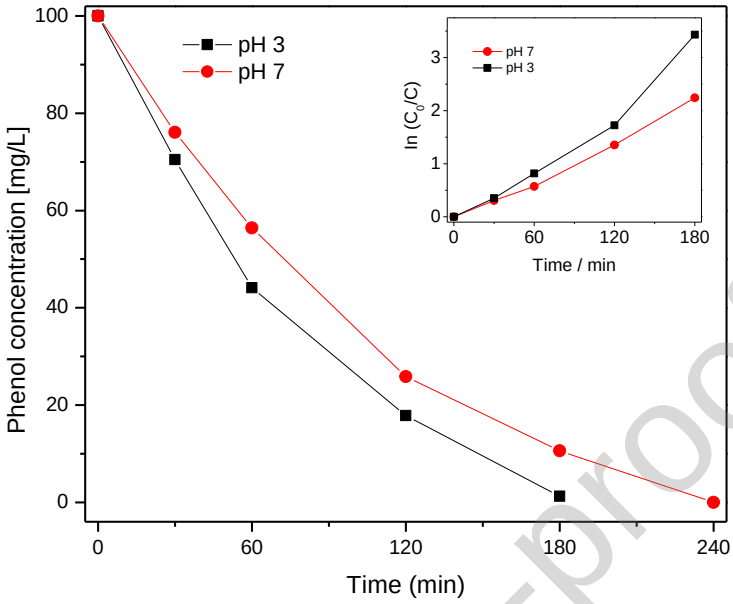

Figure 6. Comparison of phenol degradation and kinetics order. Reaction conditions: j=60 mA /cm^2, [Phenol]$_0$: 100mg/L, 0.05 M [Na_2SO_4], R: 4.7 L/min, V:3.5L, [TOC]$_0$: 118 mg/L and T: 23°C ±2

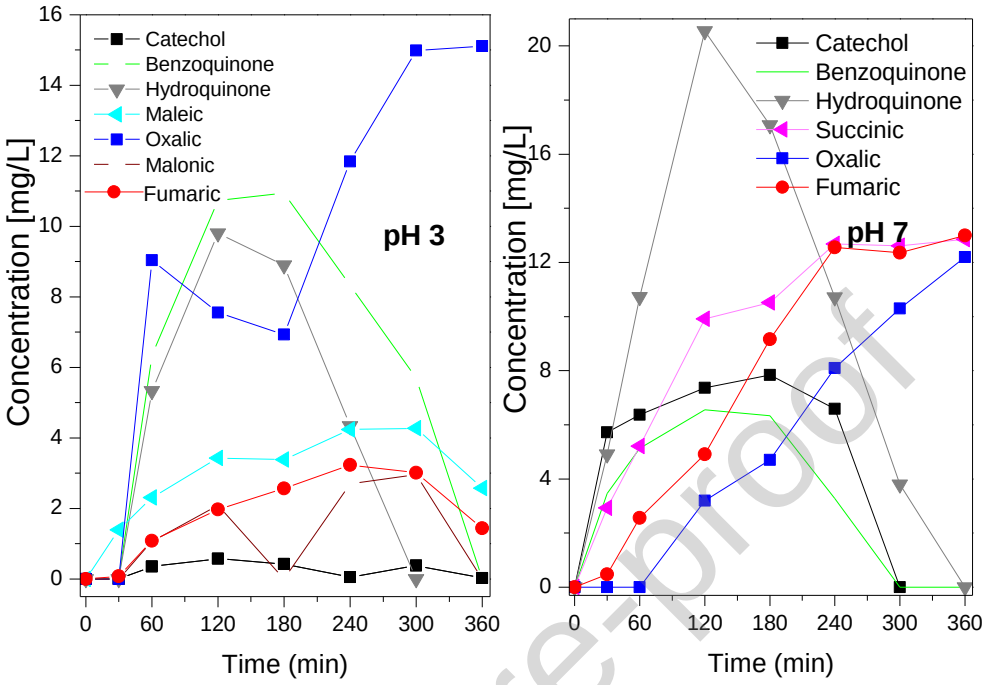

(a) (b)

Figure 7. Comparison of by-products in a) acidic and b) neutral media. Reaction conditions: J: 60 mA /cm^2, [Phenol]$_0$: 100mg/L, 0.05 M [Na_2SO_4], Q_L= 4.7 L/min, V: 3.5L. [TOC]$_0$: 118 mg/L and T= 23°C ±2.

Figure 8 depicts the effect of pH on the concentration of O_2/O_3/H_2O_2 cumulative concentration. Unlike the results obtained without phenol addition (figure 2), in this case the production and accumulation of hydrogen peroxide with time is noticeable at both pH, 3 and 7. Also at pH 3, hydrogen peroxide concentration and accumulation rate are higher than at pH 7. This can be ascribed to less consumption of this compound at pH 3 because its dissociation is lower than at pH 7, and the oxidation mechanism is mainly via molecular attack of O_3. Besides, pH 2.8 – 3 has been reported as the best range to electro-generate this oxidant [34,35]. With respect to pH 7, hydrogen peroxide concentration tends to diminish after three hours of treatment. This can be ascribed to the e-peroxone process taking over and leading to a higher H_2O_2 consumption to produce hydroxyl radicals (reaction 1) and this is reflected on the oxidation of aromatic compounds and carboxylic acids (figure 7b) and on an increase on the TOC removal rate (figure 5). Thus, it can be concluded that this technology allows to conduct the electro-peroxone process with the simultaneous electro-generation of oxygen, ozone and hydrogen peroxide, at neutral pH. Figure 9 summarizes the production of oxidant species and the plausible routes of oxidation.

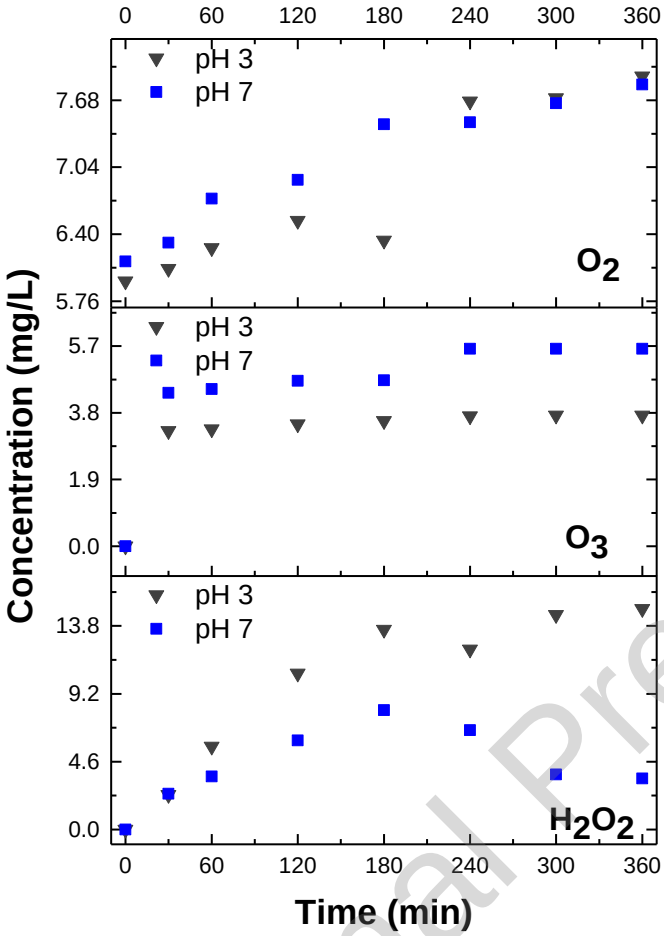

Figure 8. Effect of pH on conductive-diamond electro-generation of O_2, O_3 and H_2O_2. Reaction conditions: j=60 mA/cm^2, 0.05 M [Na_2SO_4], $[TOC]_0$=118 mg/L, Q_L= 4.7 L/min, V=3.5L and T= 23°C ±2.

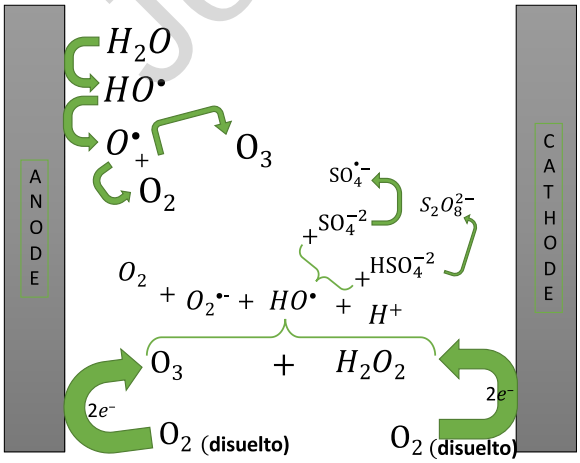

(a)

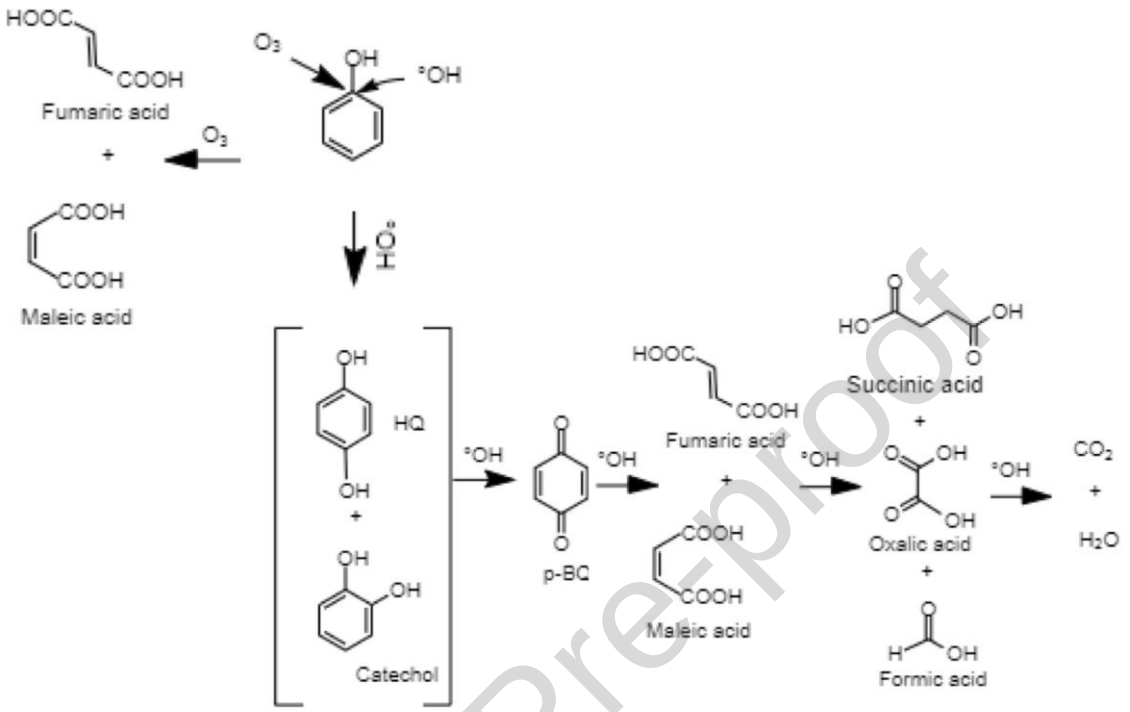

(b)

Figure 9. Production of oxidant species with BDD electrodes (a) and oxidation routes (b).

3.4 Biotoxicity study

Because the TOC removal was not 100% achieved in the assessed treatment time, it was decided to evaluate the toxicity of the treated water under pH 7.

3.4.1 Comet assay

Figure 10 shows the DNA damage, which is statistically significant in both, the positive control and the exposed to phenol group. In the case of the positive control, the increase is from 45.8 to 51% and in the case of the group exposed to phenol the increase goes from 45.7 to 52.9% with respect to the control group ($P<0.05$). It can be observed, however, that the DNA damage was significantly reduced in the treated phenol solution (EP) with respect to the positive control and the exposed to phenol group. The observed increase of 11.2-16% with respect to the control is not statistically significant ($P>0.05$). These results are in concordance to those observations made through the epifluorescence microscope and placed as insets in figure 10.

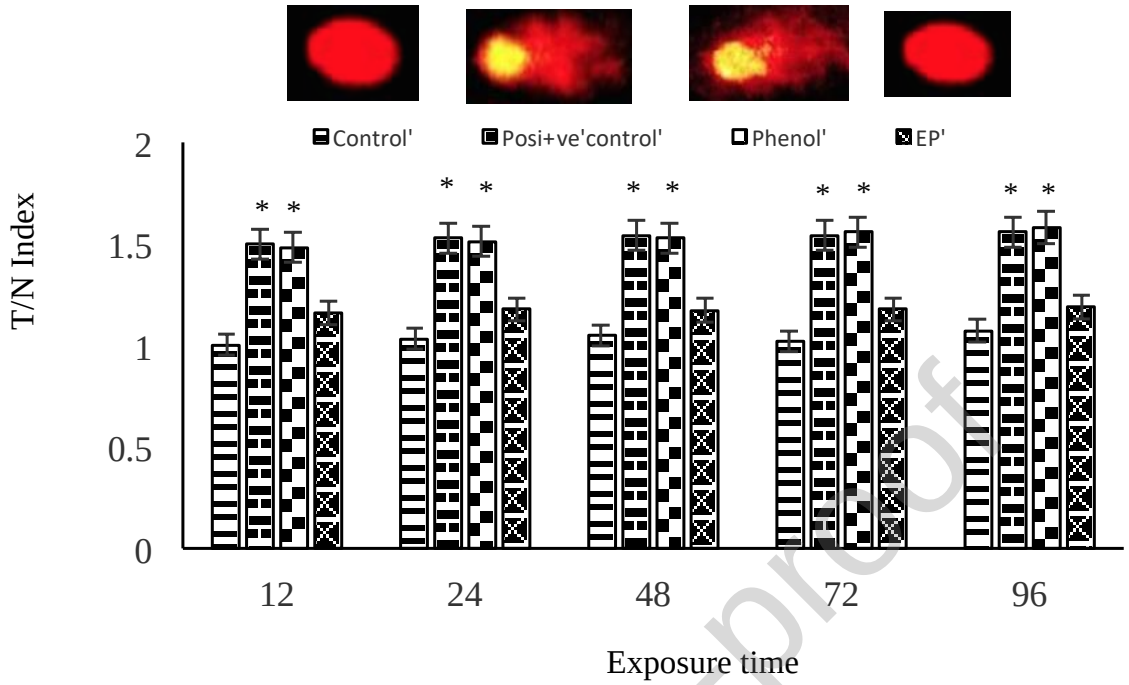

Figure10. DNA Damage

3.4.2 Micronuclei test

The results of this test are shown in figure 11. There are in the positive control group and in the exposed to phenol group, statistically significant increases with respect to the control group. In the case of the positive control group, these increases are in the range of 853-1277% and in the case of the exposed to phenol group they are in the range of 731-1233% ($P<0.05$). In the case of the treated phenol solution, a micronuclei decrease was observed with respect to the positive control group and to the exposed to phenol group. The increase respect the control group is in the range of 7.7-20%, and this was concluded not being statistically significant ($P>0.05$).

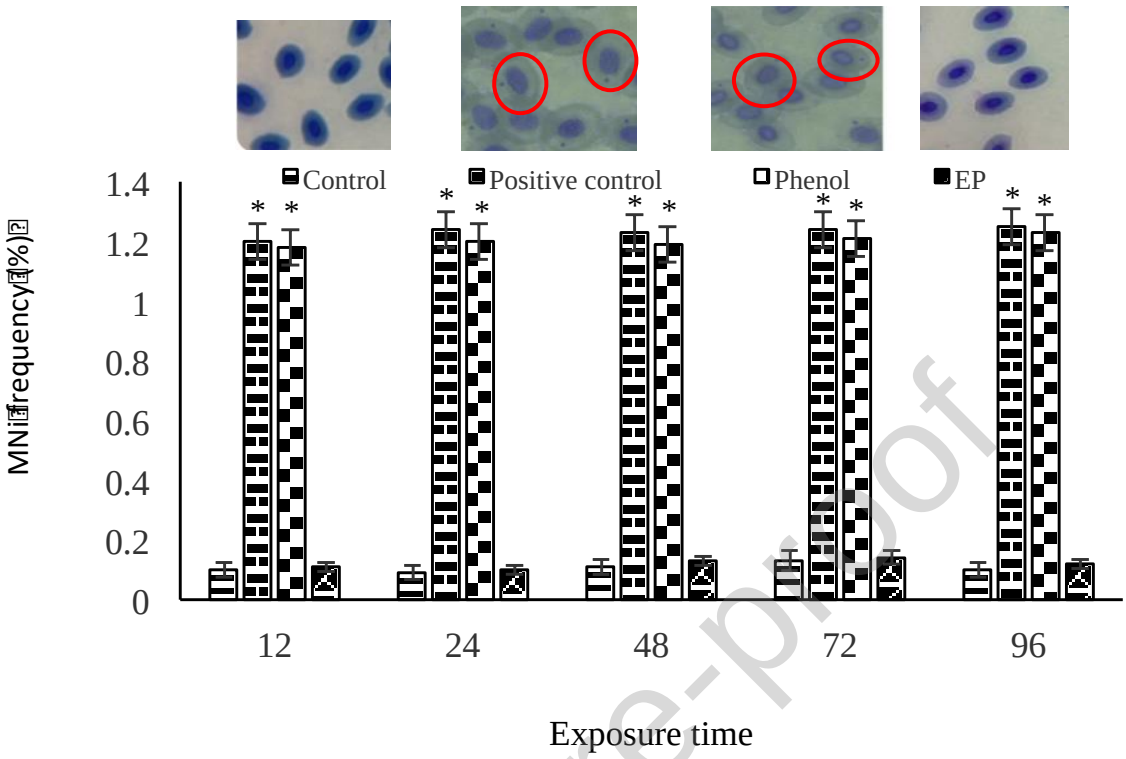

Figure 11. Micronuclei test

In this work it was decided to use single-cell electrophoresis (comet assay) as a biomarker of damage, which is a technique to assess genotoxic damage. This test detects DNA single-strand breaks (strand breaks and incomplete excision repair sites), alkali-labile sites and cross-linking, with the single-cell approach typical of cytogenetic assays [38]. In the test, it was decided to use cyclophosphamide (this is a drug from the family of alkylating agents used as an antineoplastic and immunosuppressant) as a positive control, because it has been shown to be an agent that has high genotoxic effects, besides being carcinogenic in aquatic organisms[37,38].

The model molecule used in this work was phenol, it is well known that this compound and its derivatives induce toxic responses in various fish species, the alterations that have been reported are genotoxicity, carcinogenesis, immunotoxicity, hematological damage and physiological alterations[39–43]. The mechanism through which this compound induces its toxic effects is through oxidative stress[44–48].

In addition, the micronuclei test was performed as a complimentary study. This biomarker was selected because the micronuclei (MNi) are nuclear residues produced during mitosis (or meiosis) when a fragment of a chromosome or a complete chromosome can not migrate with one of the two daughter nuclei formed. MNi can occur at different times of the event of DNA damage, depending on the kinetics of the cell cycle and the mechanism of induction [49,50]. The results obtained in this study showed that phenol at the concentration of 100 mg/L was able to induce in an important way the presence of

micronuclei in erythrocytes. These findings agree with that reported by [51] who demonstrated that phenol at different concentrations (0.7, 1.4 and 2.8 mg / L) is able to induce the production of micronuclei in *Oreochromis niloticus.*

Once the samples were treated by electroperoxone process a substantial decrease in DNA damage and MNi were observed, albeit the treatment was conducted at pH=7 and the mineralization degree was not maximum.

4. Conclusions

The Downflow Bubble Column Electrochemical Reactor allows conducting the electro-peroxone process with *in situ* production of hydrogen peroxide and ozone, without injecting air/oxygen from an external source. This reactor is able to maintain the produced gas (oxygen and/or ozone) dispersed as bubbles within the reaction system to maximize its absorption and utilization and to eliminate its waste.

The main variables affecting the overall process efficiency, in terms of TOC removal rate and/or extent, are liquid flowrate, electrolyte concentration and pH. TOC removal rate is favored at an electrolyte concentration of 0.05 M, when liquid flowrate and pH decreased. pH does exert a great effect on TOC removal rate, being higher at acidic pH. Phenolic compounds, however, can be mineralized in this system at either pH 3 or 7 with similar TOC removal extent, 75 with the former and 65 with the latter. In both cases, after 360 mins of treatment, the prevailing compounds are carboxylic acids in low concentrations.

Unlike TOC removal, phenol oxidation readily occurs at either pH, 3 or 7, and this variable determines the mechanism by which phenol is mineralized. At acidic conditions molecular ozonation attack prevails while at pH 7 the electro-peroxone process is presumed to be the main responsible of phenol mineralization. In this sense, it can also be concluded that electro-peroxone process of phenol favours hydroxylation products.

pH also affects H_2O_2, O_3 and O_2 cumulative concentrations. At pH 7 H_2O_2 consumption is higher than at pH 3 and therefore its cumulative concentration at the end of treatment is only 4 mg/L, while at pH 3 is 15 mg/L. The opposite effect was found for O_3 and O_2, although in less extent than for H_2O_2.

Although the mineralization degree is lower at pH 7 than at pH 3, conducting the electro-peroxone treatment at this condition eliminates the biotoxicity of by-products of the phenolic solution therefore water after treatment can be used for other applications.

The results at pH 7 suggest that this technology might also be applied to conduct selective oxidations and not only for water remediation.

Acknowledgements

Authors are grateful to CONACYT (Projects 168305 and 269093) for financial support. In the same way for the scholarship (CONACYT) 295553, to conduct postgraduate studies of Germán Santana-Martínez. Technical support of Citlalit Martínez Soto is also acknowledged.

References

[1] R. Natividad-Rangel, M.A.R. Rodrigo, J.J.M. Mesa, R.M.G. Espinosa, Water Remediation, J. Chem. 2017 (2017).

[2] J. Staehelin, J. Hoigne, Decomposition of ozone in water: rate of initiation by hydroxide ions and hydrogen peroxide, Environ. Sci. Technol. 16 (1982) 676–681. doi:10.1021/es00104a009.

[3] E. Peralta, R. Natividad, G. Roa, R. Marín, R. Romero, T. Pavon, A comparative study on the electrochemical production of H2O2 between BDD and graphite cathodes, Sustain. Environ. Res. (2013) 259–266. http://www.researchgate.net/publication/257873807_A_comparative_study_on_the_electrochemical_production_of_H2O2_between_BDD_and_graphite_cathodes.

[4] G. Santana-Martínez, G. Roa-Morales, E. Martin del Campo, R. Romero, B.A. Frontana-Uribe, R. Natividad, Electro-Fenton and Electro-Fenton-like with in situ electrogeneration of H2O2 and catalyst applied to 4-chlorophenol mineralization, Electrochim. Acta. 195 (2016) 246–256. doi:10.1016/j.electacta.2016.02.093.

[5] E. Isarain-Chávez, C.A. Martínez-Huitle, J.M. Peralta-Hernández, C. De la Rosa, On-site Hydrogen Peroxide Production at Pilot Flow Plant: Application to Electro-Fenton Process, 8 (2013) 3084–3094.

[6] W. Guo, Q.-L. Wu, X.-J. Zhou, H.-O. Cao, J.-S. Du, R.-L. Yin, N.-Q. Ren, Enhanced amoxicillin treatment using the electro-peroxone process: key factors and degradation mechanism, Rsc Adv. 5 (2015) 52695–52702.

[7] B. Bakheet, C. Qiu, S. Yuan, Y. Wang, G. Yu, S. Deng, J. Huang, B. Wang, Inhibition of polymer formation in electrochemical degradation of p-nitrophenol by combining electrolysis with ozonation, Chem. Eng. J. 252 (2014) 17–21. doi:https://doi.org/10.1016/j.cej.2014.04.103.

[8] X. Li, Y. Wang, S. Yuan, Z. Li, B. Wang, J. Huang, S. Deng, G. Yu, Degradation of the anti-inflammatory drug ibuprofen by electro-peroxone process, Water Res. 63 (2014) 81–93. doi:10.1016/j.watres.2014.06.009.

[9] Y. Wang, G. Yu, S. Deng, J. Huang, B. Wang, The electro-peroxone process for the abatement of emerging contaminants: Mechanisms, recent advances, and prospects, Chemosphere. 208 (2018) 640–654. doi:https://doi.org/10.1016/j.chemosphere.2018.05.095.

[10] A. Fischbacher, J. von Sonntag, C. von Sonntag, T.C. Schmidt, The •OH Radical Yield in the H2O2 + O3 (Peroxone) Reaction, Environ. Sci. Technol. 47 (2013) 9959–9964. doi:10.1021/es402305r.

[11] B. Bakheet, S. Yuan, Z. Li, H. Wang, J. Zuo, S. Komarneni, Y. Wang, Electro-peroxone treatment of Orange II dye wastewater, Water Res. 47 (2013) 6234–6243. doi:10.1016/j.watres.2013.07.042.

[12] C.A. Martínez-Huitle, E. Brillas, Decontamination of wastewaters containing synthetic organic dyes by electrochemical methods: A general review, Appl. Catal. B Environ. 87 (2009) 105–145. doi:10.1016/j.apcatb.2008.09.017.

[13] Y. Li, W. Shen, S. Fu, H. Yang, G. Yu, Y. Wang, Inhibition of bromate formation during drinking water treatment by adapting ozonation to electro-peroxone process, Chem. Eng. J. 264 (2015) 322–328. doi:10.1016/j.cej.2014.11.120.

[14] X. Li, Y. Wang, J. Zhao, H. Wang, B. Wang, J. Huang, S. Deng, G. Yu, Electro-peroxone treatment of the antidepressant venlafaxine: {Operational} parameters and mechanism, J. Hazard. Mater. 300 (2015) 298–306. doi:10.1016/j.jhazmat.2015.07.004.

[15] B. Wang, Y. Zhang, H. Ren, C. Yue, Mechanism of Mn3O4-catalyzed ozonation of drilling wastewater, Chinese J. Environ. Eng. 9 (2015) 4811–4816. https://www.scopus.com/inward/record.uri?eid=2-s2.0-84945333245&partnerID=40&md5=1a60870677fe78e959e7bf521a28619f.

[16] B. Yang, J. Deng, G. Yu, S. Deng, J. Li, C. Zhu, Q. Zhuo, H. Duan, T. Guo, Effective degradation of carbamazepine using a novel electro-peroxone process involving simultaneous electrochemical generation of ozone and hydrogen peroxide, Electrochem. Commun. 86 (2018) 26–29. doi:10.1016/j.elecom.2017.11.003.

[17] B. Marselli, J. Garcia-Gomez, P.-A. Michaud, M.A. Rodrigo, C. Comninellis, Electrogeneration of Hydroxyl Radicals on Boron-Doped Diamond Electrodes, J. Electrochem. Soc. 150 (2003) D79–D83. doi:10.1149/1.1553790.

[18] I.J. Ochuma, R.P. Fishwick, J. Wood, J.M. Winterbottom, Photocatalytic oxidation of 2,4,6-trichlorophenol in water using a cocurrent downflow contactor reactor (CDCR)., J. Hazard. Mater. 144 (2007) 627–633. doi:10.1016/j.jhazmat.2007.01.086.

[19] I.J. Ochuma, R.P. Fishwick, J. Wood, J.M. Winterbottom, Optimisation of degradation conditions of 1,8-diazabicyclo 5.4.0 undec-7-ene in water and reaction kinetics analysis using a cocurrent downflow contactor photocatalytic reactor., Appl. Catal. B-Environmental. 73 (3-4) (2007) 259–268.

[20] E. Martín del Campo, J.S. Valente, T. Pavón, R. Romero, Á. Mantilla, R. Natividad, 4-Chlorophenol Oxidation Photocatalyzed by a Calcined Mg–Al–Zn Layered Double Hydroxide in a Co-current Downflow Bubble Column, Ind. Eng. Chem. Res. 50

(2011) 11544–11552. doi:10.1021/ie200412p.

[21] G. Eisenberg, Colorimetric determination of hydrogen peroxide, Ind. Eng. Chem. Anal. Ed. 15 (1943) 327–328.

[22] H. Bader, J. Hoigné, Determination of ozone in water by the indigo method, Water Res. 15 (1981) 449–456.

[23] C. Comninellis, G. Chen, Electrochemistry for the Environment, Springer New York, New York, NY, 2010. http://www.scopus.com/inward/record.url?eid=2-s2.0-84887920143&partnerID=tZOtx3y1.

[24] P.A. Michaud, M. Panizza, L. Ouattara, T. Diaco, G. Foti, C. Comninellis, Electrochemical oxidation of water on synthetic boron-doped diamond thin film anodes, J. Appl. Electrochem. 33 (2003) 151–154. doi:10.1023/A:1024084924058.

[25] A. Thiam, R. Salazar, E. Brillas, I. Sirés, Electrochemical advanced oxidation of carbofuran in aqueous sulfate and/or chloride media using a flow cell with a RuO2-based anode and an air-diffusion cathode at pre-pilot scale, Chem. Eng. J. 335 (2018) 133–144. doi:https://doi.org/10.1016/j.cej.2017.10.137.

[26] M. Eddy, others, Wastewater engineering: treatment, disposal and reuse, McGraw-Hill, New York, USA. (1991).

[27] G. Santana-Martínez, G. Roa-Morales, E.M. Del Campo, R. Romero, B.A. Frontana-Uribe, R. Natividad, Electro-Fenton and Electro-Fenton-like with in situ electrogeneration of H<inf>2</inf>O<inf>2</inf> and catalyst applied to 4-chlorophenol mineralization, Electrochim. Acta. 195 (2016). doi:10.1016/j.electacta.2016.02.093.

[28] S. Garcia-Segura, E. Brillas, Combustion of textile monoazo, diazo and triazo dyes by solar photoelectro-Fenton: Decolorization, kinetics and degradation routes, Appl. Catal. B Environ. 181 (2016) 681–691. doi:10.1016/j.apcatb.2015.08.042.

[29] H. Olvera-Vargas, N. Oturan, M.A. Oturan, E. Brillas, Electro-Fenton and solar photoelectro-Fenton treatments of the pharmaceutical ranitidine in pre-pilot flow plant scale, Sep. Purif. Technol. 146 (2015) 127–135. doi:10.1016/j.seppur.2015.03.046.

[30] D. Amado-Piña, G. Roa-Morales, C. Barrera-Díaz, P. Balderas-Hernandez, R. Romero, E. Martín del Campo, R. Natividad, Synergic effect of ozonation and electrochemical methods on oxidation and toxicity reduction: Phenol degradation, Int. Mex. Congr. Chem. React. Eng. (IMCCRE 2016). 198 (2017) 82–90. doi:10.1016/j.fuel.2016.10.117.

[31] I. Chairez, P. Tatyana, R. Tapia, J. Vivero, Effect of pH to the Decomposition of Aqueous Phenols Mixture by Ozone, Journal of the Mexican Chemical Society, 2006.

[32] F. Beltrán, Ozone Reaction Kinetics for Water and Wastewater Systems, 1a ed., New York, Estados Unidos, 2004.

[33] O. Turkay, Z.G. Ersoy, S. Barışçı, Review—the application of an electro-peroxone process in water and wastewater treatment, J. Electrochem. Soc. 164 (2017) E94--E102. doi:10.1149/2.0321706jes.

[34] S. Garcia-Segura, Á.S. Lima, E.B. Cavalcanti, E. Brillas, Anodic oxidation, electro-{Fenton} and photoelectro-{Fenton} degradations of pyridinium- and imidazolium-based ionic liquids in waters using a {BDD}/air-diffusion cell, Electrochim. Acta. 198 (2016) 268–279. doi:10.1016/j.electacta.2016.03.057.

[35] R.C. Burgos-Castillo, I. Sirés, M. Sillanpää, E. Brillas, Application of electrochemical advanced oxidation to bisphenol {A} degradation in water. {Effect} of sulfate and chloride ions, Chemosphere. 194 (2018) 812–820. doi:10.1016/j.chemosphere.2017.12.014.

[36] L.D. Knopper, J.P. McNamee, Use of the comet assay in environmental toxicology, in: Environ. Genomics, Springer, 2008: pp. 171–184.

[37] M. Novak, B. Žegura, B. Modic, E. Heath, M. Filipič, Cytotoxicity and genotoxicity of anticancer drug residues and their mixtures in experimental model with zebrafish liver cells, Sci. Total Environ. 601–602 (2017) 293–300. doi:https://doi.org/10.1016/j.scitotenv.2017.05.115.

[38] T.G. Fonseca, M. Auguste, F. Ribeiro, C. Cardoso, N.C. Mestre, D.M.S. Abessa, M.J. Bebianno, Environmental relevant levels of the cytotoxic drug cyclophosphamide produce harmful effects in the polychaete Nereis diversicolor, Sci. Total Environ. 636 (2018) 798–809. doi:https://doi.org/10.1016/j.scitotenv.2018.04.318.

[39] L. Taysse, D. Troutaud, N.A. Khan, P. Deschaux, Structure-activity relationship of phenolic compounds (phenol, pyrocatechol and hydroquinone) on natural lymphocytotoxicity of carp (Cyprinus carpio), Toxicology. 98 (1995) 207–214. doi:https://doi.org/10.1016/0300-483X(94)03011-P.

[40] T. Tsutsui, N. Hayashi, H. Maizumi, J. Huff, J.C. Barrett, Benzene-, catechol-, hydroquinone- and phenol-induced cell transformation, gene mutations, chromosome aberrations, aneuploidy, sister chromatid exchanges and unscheduled DNA synthesis in Syrian hamster embryo cells, Mutat. Res. Mol. Mech. Mutagen. 373 (1997) 113–123. doi:https://doi.org/10.1016/S0027-5107(96)00196-0.

[41] M.C.L. Erbe, W.A. Ramsdorf, T. Vicari, M.M. Cestari, Toxicity evaluation of water samples collected near a hospital waste landfill through bioassays of genotoxicity piscine micronucleus test and comet assay in fish Astyanax and ecotoxicity Vibrio fischeri and Daphnia magna, Ecotoxicology. 20 (2011) 320–328.

[42] H.S.H.S. Remya Varadarajan, J. Jose, B. Philip, Sublethal effects of phenolic

compounds on biochemical, histological and ionoregulatory parameters in a tropical teleost fish Oreochromis mossambicus (Peters), (n.d.).

[43] W. Duan, F. Meng, H. Cui, Y. Lin, G. Wang, J. Wu, Ecotoxicity of phenol and cresols to aquatic organisms: A review, Ecotoxicol. Environ. Saf. 157 (2018) 441–456. doi:https://doi.org/10.1016/j.ecoenv.2018.03.089.

[44] H. Roche, G. Bogé, In vivo effects of phenolic compounds on blood parameters of a marine fish (Dicentrarchus labrax), Comp. Biochem. Physiol. Part C Pharmacol. Toxicol. Endocrinol. 125 (2000) 345–353. doi:https://doi.org/10.1016/S0742-8413(99)00119-X.

[45] I.M. Avilez, T.S.F. Hori, L.C. de Almeida, A. Hackbarth, J. da C.B. Neto, V.L.F. da C. Bastos, G. Moraes, Effects of phenol in antioxidant metabolism in matrinxã, Brycon amazonicus (Teleostei; Characidae), Comp. Biochem. Physiol. Part C Toxicol. Pharmacol. 148 (2008) 136–142. doi:https://doi.org/10.1016/j.cbpc.2008.04.008.

[46] T.S.F. Hori, I.M. Avilez, L.K. Inoue, G. Moraes, Metabolical changes induced by chronic phenol exposure in matrinxã Brycon cephalus (teleostei: characidae) juveniles, Comp. Biochem. Physiol. Part C Toxicol. Pharmacol. 143 (2006) 67–72. doi:https://doi.org/10.1016/j.cbpc.2005.12.004.

[47] A.A. Charan, A.I. Charan, O.M.P. Verma, S.S. Naushad, others, Profiling of antioxidant enzymes in cat fish (Clarias batrachus) exposed to phenolic compounds., Asian J. Bio Sci. 10 (2015) 6–14.

[48] K. Cho, C.-H. Lee, K. Ko, Y.-J. Lee, K.-N. Kim, M.-K. Kim, Y.-H. Chung, D. Kim, I.-K. Yeo, T. Oda, Use of phenol-induced oxidative stress acclimation to stimulate cell growth and biodiesel production by the oceanic microalga Dunaliella salina, Algal Res. 17 (2016) 61–66. doi:https://doi.org/10.1016/j.algal.2016.04.023.

[49] V. V Arkhipchuk, N.N. Garanko, Using the nucleolar biomarker and the micronucleus test on in vivo fish fin cells, Ecotoxicol. Environ. Saf. 62 (2005) 42–52. doi:https://doi.org/10.1016/j.ecoenv.2005.01.001.

[50] M. Hayashi, The micronucleus test—most widely used in vivo genotoxicity test—, Genes Environ. 38 (2016) 18.

[51] N.S. Gad, A.S. Saad, Effect of environmental pollution by phenol on some physiological parameters of Oreochromis niloticus, Glob. Vet. 2 (2008) 312–319.

Graphical abstract

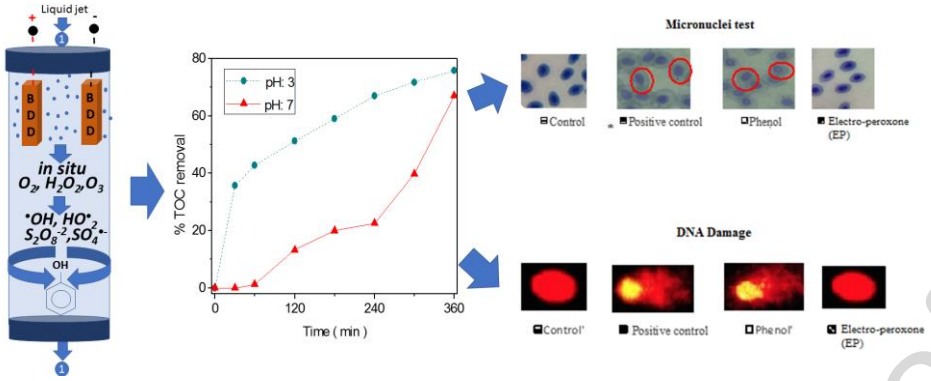

CRediT authorship contribution statement

G. Santana and E. Peralta performed experiments regarding the oxidation of phenol. L. Gómez-Olivan conducted the experiments and analysis regarding toxicity. G. Santana, R. Romero, G. Roa and R. Natividad conducted the writing, analysis and editing.

Declaration of interests

☒ The authors declare that they have no known competing financial interests or personal relationships that could have appeared to influence the work reported in this paper.

☐The authors declare the following financial interests/personal relationships which may be considered as potential competing interests: